Atomic-Layer Alignment Tuning for Giant Perpendicular Magnetocrystalline Anisotropy of 3*d* Transition-Metal Thin Films

K. Hotta,[1] K. Nakamura,[1,*] T. Akiyama,[1] T. Ito,[1] T. Oguchi,[2] and A. J. Freeman[3]

[1]*Department of Physics Engineering, Mie University, Tsu, Mie 514-8507, Japan*
[2]*The Institute of Scientific and Industrial Research, Osaka University, Ibaraki, Osaka 567-0047, Japan*
[3]*Department of Physics and Astronomy, Northwestern University, Evanston, Illinois 60208, USA*

(Received 27 February 2013; revised manuscript received 20 May 2013; published 28 June 2013)

The magnetocrystalline anisotropy (MA) of Fe-based transition-metal thin films, consisting of only magnetic 3*d* elements, was systematically investigated from full-potential linearized augmented plane-wave calculations. The results predict that giant MA with a perpendicular magnetic easy axis (PMA) can be achieved by tuning the atomic-layer alignments in an Fe-Ni thin film. This giant PMA arises from the spin-orbit coupling interaction between occupied and unoccupied Ni $d_{x^2-y^2,xy}$ bands crossing the Fermi level. A promising 3*d* transition-metal thin film for the MgO-based magnetic tunnel junctions with the giant PMA was, thus, demonstrated.

DOI: 10.1103/PhysRevLett.110.267206 PACS numbers: 75.30.Gw, 71.20.Be, 75.70.Ak

Much interest in magnetic tunnel junctions (MTJs) with a perpendicular magnetic easy axis [perpendicular magnetocrystalline anisotropy (PMA)], consisting of ferromagnetic transition-metal thin films with a MgO barrier, has rapidly increased in ultrahigh density and nonvolatile spin electronics [1,2]. Currently, experimental efforts have successfully synthesized artificial transition-metal thin films including rare-earth and noble (Pt, Pd) elements [3–9], which exhibit large PMA that promisingly overcomes the shape in-plane magnetic anisotropy and thermal fluctuations on a device level.

In parallel, efforts for searching promising PMA materials with no requirement of such additional rare-earth or noble elements have remained a great challenge [10–14]. A key feature dealing with large PMA systems of the 3*d* transition-metals is in understanding and controlling the spin-orbit coupling interaction (SOC), $H_{\rm soc} = \xi(r)\sigma\ell$, in ferromagnetic thin films and at surfaces and interfaces [15]. For the 3*d* transition-metals, since the SOC strength, $\xi(r)$, is weak due to the weak Coulomb potential near the 3*d* atom's nucleus, the magnetocrystalline anisotropy (MA) energy generally reduces to be 10^{-3} meV in cubic bulk systems, i.e., much smaller than that in rare-earth or noble materials. However, at surfaces and interfaces, the MA energy reaches as much as 10^{-1} meV, induced by symmetry lowering and orbital localization at surfaces or interfaces. Remarkably, recent findings of the PMA in Fe/MgO(001) [16,17] and CoFeB/MgO(001) [2,18,19] interfaces, where a weak Fe d_{z^2}-O p_z hybridization at the interface enhances the PMA, have led to an important avenue toward the successful MTJ devices with the PMA.

In our search for PMA materials, the MA of Fe-based transition-metal thin films, consisting of only magnetic 3*d* elements of Mn, Fe, Co, and Ni, were systematically investigated by means of first principles full-potential linearized augmented plane-wave (FLAPW) method [20,21]. As a major achievement, here, we find that apart from the interfacial PMA [2,16–18], a giant PMA can be achieved by tuning the atomic-layer alignments in an Fe-Ni film, arising from the SOC between occupied and unoccupied Ni $d_{x^2-y^2,xy}$ bands crossing the Fermi level ($E_{\rm F}$). Thus, a tailored 3*d* transition-metal thin film for the MTJs with giant PMA, without the rare-earth or noble elements, was demonstrated.

Calculations were performed based on generalized gradient approximation (GGA) [22] by using the FLAPW method with a single slab geometry, in which the core states are treated fully relativistically and the valence states are treated in the scalar relativistic approximation (SRA), i.e., without SOC. The LAPW functions with a cutoff of $|\mathbf{k} + \mathbf{G}| \leq 3.9$ a.u. and muffin-tin (MT) sphere radii of 2.2 a.u. for Mn, Fe, Co, and Ni atoms are used, where the angular-momentum expansion inside the MT spheres is truncated at $\ell = 8$ for the wave functions, charge and spin densities, and potential.

To determine the MA, the second variational method [23] for treating the SOC was performed by using the calculated eigenvectors in the SRA, and the MA energy, $E_{\rm MA}$, is determined by the force theorem [24,25], which is defined as the energy eigenvalue difference for the magnetization oriented along the in-plane and the perpendicular directions to the film plane. The use of 7056 special k points in the two-dimensional Brillouin zone (BZ) was sufficient to suppress numerical fluctuations less than 0.01 meV in the $E_{\rm MA}$.

As models of the thin films, as shown in Fig. 1, we employed five- and seven-layer slabs with a bcc-like-layer stacking, where both sides of the films are terminated by Fe layers for taking an advantage to include the Fe/MgO interfaces. Possible atomic-layer alignments with the Fe and the other 3*d* elements (Mn, Co, and Ni), type I, II, and III structures for the five-layer film and type I–VI structures for the seven-layer film, are considered.

 © 2013 American Physical Society

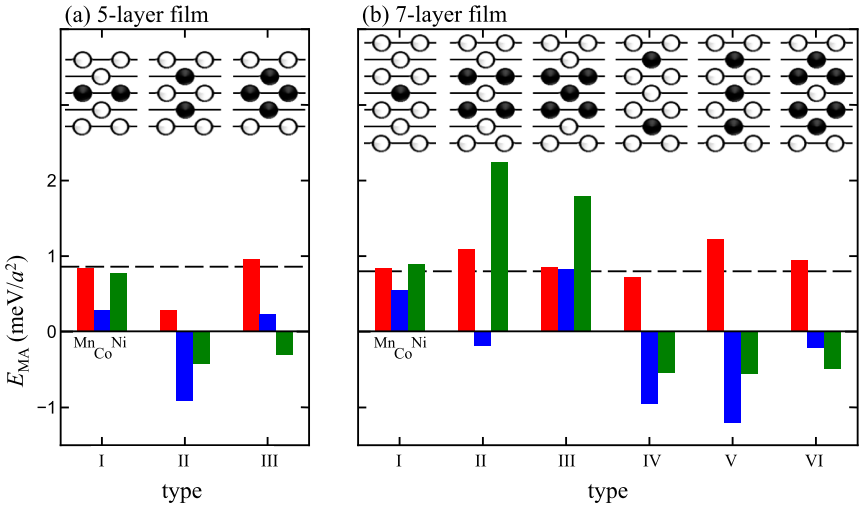

FIG. 1 (color online). Calculated E_{MA} for (a) five and (b) seven-layer slabs of Fe-based transition-metal thin films with a bcc-like-layer stacking with Mn, Co, and Ni layers, where both sides of the films are terminated by Fe layers. Dashed horizontal lines represent results for pure Fe films. In the insets, models employed are illustrated, type I, II, and III structures for the five-layer film and type I–VI structures for the seven-layer film, where open and solid circles represent Fe and the other 3*d* elements (Mn, Co, and Ni), respectively.

For simplicity, symmetric alignments along the z axis were imposed. For the magnetic structure, an ferromagnetic state with the lowest energy state, except an antiparallel Mn moment at the center layer in the type III Fe-Mn structure, is considered. The in-plane lattice constant is assumed to match the calculated value of bulk MgO, $a = 3.01$ Å, and all atomic positions are fully optimized by atomic force calculations.

The calculated E_{MA} are summarized in Fig. 1, where the E_{MA} of the pure Fe film is also given by the dashed horizontal lines. The pure Fe films have a positive E_{MA}, 0.86 and 0.80 meV/a^2 for both five- and seven-layer films, which indicates that the magnetization energetically favors pointing in the perpendicular (PMA) direction. In the five-layer film, for all Fe-Mn, Fe-Co, and Fe-Ni films, the E_{MA} tends to decrease or have negative values compared to that of the pure Fe film.

Interestingly, in the seven-layer film, we observed a large positive E_{MA}, 2.24 and 1.79 meV/a^2, for the type II and III Fe-Ni structures [26], which are larger than that in the pure Fe film by a factor of more than two. This notes that the atomic-layer ordering of alternating Fe and Ni layers in the type II structure enhances the PMA over that in the type III structure. The Fe double layers on both sides of the film in the type II Fe-Ni structure are also found to need for the PMA. This was confirmed from the fact that the type V Fe-Ni structure, with the same Fe and Ni layer ordering but terminated by Fe monolayers, has a negative value of the E_{MA}, −0.55 meV/a^2.

In addition, we carried out calculations for the type II Fe-Ni structure covered by double layers of MgO, $(MgO)_2/Fe_2/Ni/Fe/Ni/Fe_2/(MgO)_2$, and found that the E_{MA} results in 2.99 meV/a^2, i.e., an increase by 0.75 meV/a^2 over that without the MgO, due to the interfacial PMA at the Fe/MgO interfaces [16,17]. The E_{MA} value, that corresponds to 5.42×107 erg/cm^3, exceeds enough over the shape MA energy, 1.5×10^7 erg/cm^3, of the film with a magnetization of 1.54×10^3 emu/cm^3. Thus, a promising 3*d* transition-metal thin film for the MgO-based MTJs with the giant PMA was tailored.

Experimentally, the film with the bcc-like-layer stacking of the Ni layer on Fe(001), as seen in the type II Fe-Ni structure, may be fabricated. From the fact that the bcc-like B2 structure in bulk FeNi is only 0.15 eV/atom higher in energy than the fcc-like $L1_0$ structure [27], the bcc-like growth is expected in a thin enough film. Furthermore, a constraint of the in-plane lattice constant from the Fe (or MgO in the present case) substrate may avoid the fcc-like-layer stacking, since the lattice constant of the $L1_0$ structure (2.51 Å) is too small compared to that of the substrate. Indeed, bcc Ni overlayers, up to three monolayers, were epitaxially grown on bcc Fe(001) in experiments [28]. Defects in films to the PMA may be further inevitable in experiments. As in Fig. 1(b), an atomic disorder (different layer stacking) may give rise to a large variation in the E_{MA}. It, however, notes that when the films are terminated by more than Fe double layers, the E_{MA} always remains in positive values, as mentioned above; it may be valid even if the atomic disorder is introduced.

To verify the giant PMA in the type II Fe-Ni structure, we extended our calculations to thicker films with the alternate ordering of the Fe and Ni layers terminated by the Fe double layers. Results are shown by solid circles in Fig. 2, where those of the pure Fe films are also presented. The pure Fe films always have positive E_{MA} and almost no dependence on the film thickness, which indicates that the E_{MA} comes from the surface contribution. For the present system, the E_{MA} increases significantly, by 1.5 meV/a^2 in

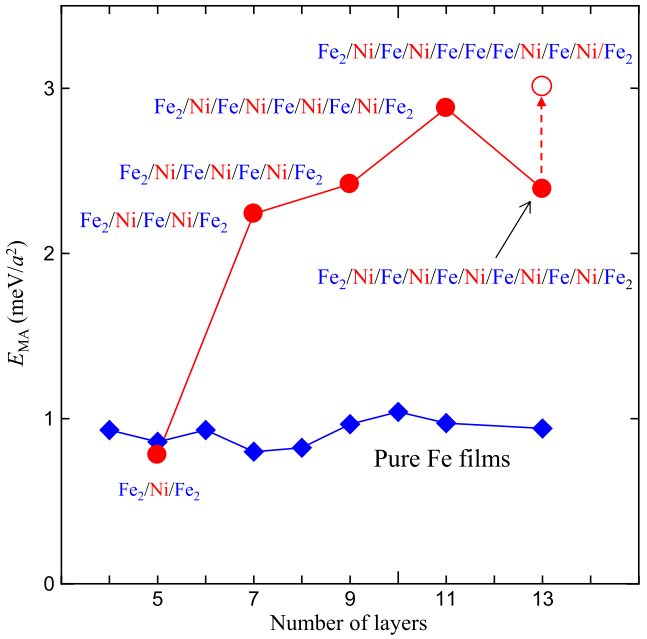

FIG. 2 (color online). Calculated E_{MA} of Fe-Ni films (circles) as a function of the film thickness. Solid circles represent results for films with an alternate ordering of Fe and Ni layers terminated by Fe double layers on both sides of the films and an open circle for a film Fe_2/Ni/Fe/Ni/Fe/Fe/Fe/Ni/Fe/Ni/Fe_2. Notations illustrate atomic-layer orderings of the Fe and Ni layers in the films. Results of the pure Fe films are shown by solid diamonds.

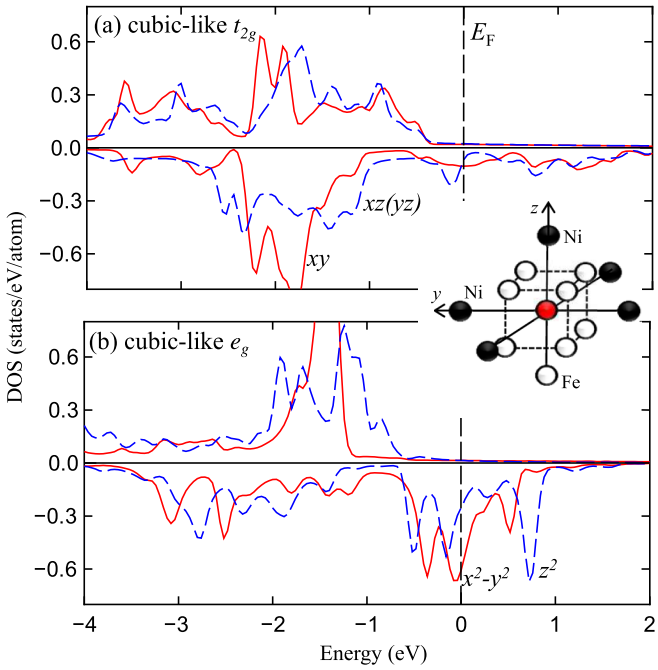

FIG. 3 (color online). Calculated orbital-decomposed DOS in the Ni MT sphere of type II Fe-Ni structure, Fe_2/Ni/Fe/Ni/Fe_2, where (a) and (b) show those of the cubiclike t_{2g} and e_g states; the former (latter) is composed of $d_{xz(yz)}$ and d_{xy} (d_{z^2} and $d_{x^2-y^2}$). As shown in an inset, the Ni atom locates in a C_{4v} symmetry site, surrounded by eight nearest-neighbor Fe atoms, four Ni atoms on the same plane, and one Ni (Fe) atom above (below).

the seven-layer film over that in the five-layer film, but the E_{MA} almost saturates when the film thickness increases further [29]. With the thirteen-layer model where the Ni layer at the center is replaced by an Fe layer, i.e., Fe_2/Ni/Fe/Ni/Fe/Fe/Fe/Ni/Fe/Ni/Fe_2, the E_{MA} is found to increase up to 3 meV/a^2, as shown by an open circle in Fig. 2. Thus, the bcc-like-layer stacking of Fe_2/Fe/Ni/Fe/Ni/Fe_2 gives rise to the PMA.

Figure 3 shows the partial density of states (DOS) in the Ni MT sphere of the type II Fe-Ni structure, Fe_2/Ni/Fe/Ni/Fe_2, where the DOS around E_F arises from the minority-spin state while the majority spin state is almost fully occupied and is located from 0.5 to 4 0 eV below E_F. As illustrated in the inset, the Ni atom locates at a C_{4v} symmetry site, surrounded by eight nearest-neighbor Fe atoms, four Ni atoms on the same plane, and one Ni (Fe) atom above (below). The ligand field from the nearest-neighbor Fe atoms splits the d state into the cubic-like t_{2g} and e_g levels, and the tetragonal symmetry further splits the t_{2g} state into two irreducible representations, a singlet b_2 (d_{xy}) and a doublet e ($d_{xz,yz}$), and the e_g state into two irreducible representations, singlets a_1 (d_{z^2}) and b_1 ($d_{x^2-y^2}$).

In the minority-spin state in Fig. 3, three characteristic features are observed. First, the cubic-like t_{2g} state, i.e., the $d_{xz,yz}$ and d_{xy} orbitals, hybridize with the nearest-neighbor Fe atoms, so these bands with a bonding character are pushed down in energy from 1.0 to 2.5 eV below E_F. Since the antibonding state is mainly attributed in the counterpart Fe atoms, the DOS of the Ni $d_{xz,yz}$ and d_{xy} orbitals around E_F is small. Secondly, for the cubic-like e_g state, the hybridization between neighboring Ni atoms with the $d_{x^2-y^2}$ orbitals on the same plane pushes the antibonding state close to E_F in energy. Finally, the DOS peaks of the antibonding d_{z^2} state shift above and below E_F so as to reduce the DOS at E_F due to the Ni and Fe atoms above and below along the z axis.

The E_{MA} contribution on the $\mathbf{k}$ space, $E_{MA}(\mathbf{k})$, of the type II Fe-Ni structure is shown in Fig. 4(a). Although there is the negative contribution to the E_{MA}, most of the BZ shows the positive contribution that favors energetically the PMA. Particularly, a very large positive contribution appears close to around $5/12(\bar{X} + \bar{M})$, as indicated by an arrow in the figure. With a correlation in the $E_{MA}(\mathbf{k})$ and the minority-spin band structure from $\bar{\Gamma}$ to $1/2(\bar{X} + \bar{M})$, as shown in Figs. 4(b) and 4(c), the large positive peak in the $E_{MA}(\mathbf{k})$ is identified from the SOC between the $d_{x^2-y^2}$ and d_{xy} bands crossing E_F.

According to perturbation theory [30], the SOC between occupied and unoccupied states with the same (different) m magnetic quantum number through the ℓ_z (ℓ_x) operator gives a positive (negative) contribution to the E_{MA}, as

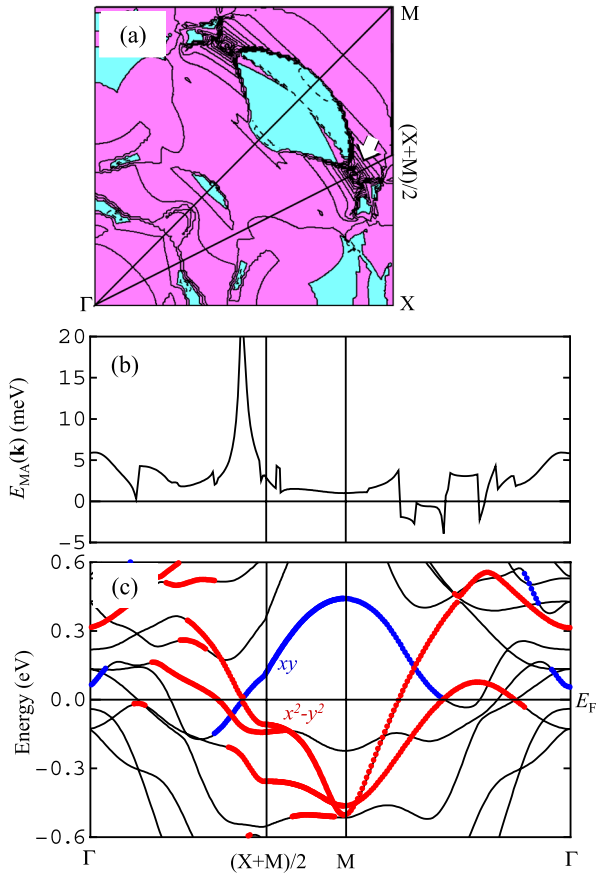

FIG. 4 (color online). (a) Calculated E_{MA} contribution in $\mathbf{k}$ space, $E_{MA}(\mathbf{k})$, of type II Fe-Ni structure, $Fe_2/Ni/Fe/Ni/Fe_2$. Solid lines (pink area) and dashed lines (light blue) represent positive and negative contributions to the E_{MA}, respectively. An arrow (white) points to a $\mathbf{k}$ position that has a largest positive contribution. (b) Calculated $E_{MA}(\mathbf{k})$ and (c) minority-spin band structure along directions drawn by solid lines in (a). In (c), solid circles represent bands having components of $d_{x^2-y^2}$ [solid circles (red)] and d_{xy} [solid circles (blue)] orbitals (possessing more than 5%) in the Ni MT sphere.

$$E_{MA} \approx \xi^2 \sum_{o,u} \frac{|\langle o \mid \ell_z \mid u\rangle|^2 - |\langle o \mid \ell_x \mid u\rangle|^2}{\epsilon_u - \epsilon_o}, \quad (1)$$

where o (u) and ϵ_o (ϵ_u) represent eigenstates and eigenvalues, respectively, of occupied (unoccupied) minority-spin states. In the present system, at around $5/12(\bar{X} + \bar{M})$, the ℓ_z matrix of the first term in Eq. (1) leads to a large positive value in the E_{MA}, since the eigenstates ($d_{x^2-y^2,xy}$) have the largest $|m|$ value (2) and a small energy splitting between the occupied and occupied states increases the E_{MA} significantly through the denominator in Eq. (1). In contrast, the ℓ_x matrix of the second term in Eq. (1), i.e., $\langle 0 \mid \ell_x \mid \pm 1\rangle$ and $\langle \pm 2 \mid \ell_x \mid \pm 1\rangle$, has a small contribution to the E_{MA}, since less DOS of the $d_{m=\pm 1}$ ($d_{xz,yz}$) components appears around E_F, as pointed out in Fig. 3(a). Thus, the SOC between the Ni $d_{x^2-y^2,xy}$ bands crossing E_F leads to the giant PMA.

In summary, we systematically investigated the PMA of the Fe-based transition-metal thin films, consisting of only magnetic $3d$ elements, by means of first-principles FLAPW calculations. As demonstrated by possible atomic-layer alignments with the Fe and the other $3d$ elements (Mn, Co, and Ni) in the five- and seven-layer films, we found that the large PMA can be achieved by tuning the atomic-layer alignments in the Fe-Ni film; i.e., the bcc-like-layer stacking of $Fe_2Ni/Fe/Ni/Fe_2$ plays a key role. This was further confirmed from calculations for the thicker films, and the calculated E_{MA} reaches as much as 3 meV/a^2. The calculated band structure shows that the giant PMA arises from the SOC between the occupied and unoccupied Ni $d_{x^2-y^2,xy}$ bands crossing E_F.

Work at Mie University was supported by a Grant-in-Aid for Scientific Research (20540334) and Young Researcher Overseas Visits Program for Vitalizing Brain Circulation (R2214) from the Japan Society for the Promotion of Science, and was performed under the Cooperative Research Program of "Network Joint Research Center for Materials and Devices" at Osaka University. Computations were performed at ISSP, University of Tokyo. Work at Northwestern University was supported by U.S. Department of Energy (DE-FG02-05ER45372).

*kohji@phen.mie-u.ac.jp

[1] A. D. Kent, Nat. Mater. **9**, 699 (2010).
[2] S. Ikeda, K. Miura, H. Yamamoto, K. Mizunuma, H. D. Gan, M. Endo, S. Kanai, J. Hayakawa, F. Matsukura, and H. Ohno, Nat. Mater. **9**, 721 (2010).
[3] H. Ohmori, T. Hatori, and S. Nakagawa, J. Appl. Phys. **103**, 07A911 (2008).
[4] M. Nakayama, T. Kai, N. Shimomura, M. Amano, E. Kitagawa, T. Nagase, M. Yoshikawa, T. Kishi, S. Ikegawa, and H. Yoda, J. Appl. Phys. **103**, 07A710 (2008).
[5] T. Shima, T. Moriguchi, S. Mitani, and K. Takanashi, Appl. Phys. Lett. **80**, 288 (2002).
[6] G. Kim, Y. Sakuraba, M. Oogane, Y. Ando, and T. Miyazaki, Appl. Phys. Lett. **92**, 172502 (2008).
[7] B. Carvello, C. Ducruet, B. Rodmacq, S. Auffret, E. Gautier, G. Gaudin, and B. Dieny, Appl. Phys. Lett. **92**, 102508 (2008).
[8] K. Mizunuma, S. Ikeda, J. H. Park, H. Yamamoto, H. Gan, K. Miura, H. Hasegawa, J. Hayakawa, F. Matsukura, and H. Ohno, Appl. Phys. Lett. **95**, 232516 (2009).
[9] K. Yakushiji, T. Saruya, H. Kubota, A. Fukushima, T. Nagahama, S. Yuasa, and K. Ando, Appl. Phys. Lett. **97**, 232508 (2010).
[10] G. H. O. Daalderop, P. J. Kelly, and F. J. A. den Broeder, Phys. Rev. Lett. **68**, 682 (1992).
[11] K. Nakamura, M. Kim, A. J. Freeman, L. Zhong, and J. Fernandez-de-Castro, IEEE Trans. Magn. **36**, 3269 (2000).

[12] P. Ravindran, A. Kjekshus, H. Fjellvaag, P. James, L. Nordstrom, B. Johansson, and O. Eriksson, Phys. Rev. B **63**, 144409 (2001).
[13] T. Shima, M. Okamura, S. Mitani, and K. Takanashi, J. Magn. Magn. Mater. **310**, 2213 (2007).
[14] T. Burkert, L. Nordström, O. Eriksson, and O. Heinonen, Phys. Rev. Lett. **93**, 027203 (2004).
[15] R. Wu and A. J. Freeman, J. Magn. Magn. Mater. **200**, 498 (1999).
[16] R. Shimabukuro, K. Nakamura, T. Akiyama, and T. Ito, Physica (Amsterdam) **42E**, 1014 (2010).
[17] K. Nakamura, T. Akiyama, T. Ito, M. Weinert, and A. J. Freeman, Phys. Rev. B **81**, 220409 (2010).
[18] H. X. Yang, M. Chshiev, B. Dieny, J. H. Lee, A. Manchon, and K. H. Shin, Phys. Rev. B **84**, 054401 (2011).
[19] The PMA at the CoFeB/MgO interface in experiments (Ref. [2]) is expected to contribute mainly in the interfacial Fe-O hybridization, according to results in Ref. [18].
[20] E. Wimmer, H. Krakauer, M. Weinert, and A. J. Freeman, Phys. Rev. B **24**, 864 (1981).
[21] M. Weinert, E. Wimmer, and A. J. Freeman, Phys. Rev. B **26**, 4571 (1982).
[22] J. P. Perdew, K. Burke, and M. Ernzerhof, Phys. Rev. Lett. **77**, 3865 (1996).
[23] C. Li, A. J. Freeman, H. J. F. Jansen, and C. L. Fu, Phys. Rev. B **42**, 5433 (1990).
[24] M. Weinert, R. E. Watson, and J. W. Davenport, Phys. Rev. B **32**, 2115 (1985).
[25] G. H. O. Daalderop, P. J. Kelly, and M. F. H. Schuurmans, Phys. Rev. B **41**, 11 919 (1990).
[26] The validity of the force theorem was confirmed by self-consistent total energy calculations including the SOC, where the E_{MA} in the self-consistent calculations is 2.40 meV$/a^2$ for the type II Fe-Ni structure.
[27] Y. Mishin, M. J. Mehl, and D. A. Papaconstantopoulos, Acta Metall. Mater. **53**, 4029 (2005).
[28] A. V. Mijiritskii, P. J. M. Smulders, V. Y. Chumamov, O. C. Rogojanu, M. A. James, and D. O. Boerma, Phys. Rev. B **58**, 8960 (1998).
[29] In films capped by double-layers of MgO, the E_{MA} was confirmed to always increase over that without the MgO, e.g., by 0.10 and 0.31 meV$/a^2$ for the nine and eleven-layer films and by 0.36 and 0.19 meV$/a^2$ for the type I and III structures in Fig. 1(b), where the magnitude depends on the film thickness and the layer-stacking alignment.
[30] D. S. Wang, R. Wu, and A. J. Freeman, Phys. Rev. B **47**, 14 932 (1993).